Optimal Torque Distribution Control Strategy for Parallel Hybrid Electric Urban Buses

YUANGJUN HUANG, CHENGLIANG YIN, JIANWU ZHANG
School of Mechanical Engineering
Shanghai Jiao Tong University
800 Dongchuan Rd., Shanghai, 200240
CHINA
victor_huangyj@sjtu.edu.cn

Abstract: - A novel parallel hybrid electric urban bus (PHEUB) configuration consisting of an extra one-way clutch and an automatic mechanical transmission (AMT) is taken as the study subject. Feed-forward computer simulation model of the PHEUB was developed in the system simulation software MATLAB/Simulink environment. The bench test results for the key components of the hybrid powertrain are treated as reliable reference in the modeling. A logic threshold torque distribution control strategy incorporating with an instantaneously optimization algorithm is proposed for the investigated PHEUB. The aim is to optimize the fuel economy and balance the battery state-of-charge (SOC), while satisfying the vehicle performance and drivability requirements at all times. Simulation results for the behaviors of the engine, motor and battery illustrates the potential of the proposed control strategy in terms of fuel economy and in keeping the deviations of battery SOC at a low level. The presented control strategy has been applied to the experimental hybrid bus and it is shown from the monitoring and testing that the control functions are practical.

Key-Words: - Hybrid electric vehicles, Fuel economy, Modeling and simulation, Optimal Control strategy, Logic torque distribution control strategy, Operating mode control.

1 Introduction

Along with the increasing of the vehicles quantity, people have paid more attentions on the problems of environmental protection and energy shortage. Hybrid electric vehicle (HEV), which incorporates the advantages of both the battery electric vehicle and the conventional vehicle, has attached more and more attentions for its merits of high fuel efficiency, low emissions, long driving range, and moderate price [1,2].

The main feature of a parallel HEV is that its powertrain is primarily comprised by the engine and the electric drive system. This means an additional degree of freedom is available to satisfy power demands from the driver. Since the power can be split between thermal and electrical paths, the performance of the parallel HEV system strongly depends on the control of this power split. The optimal distribution of the power is the kernel part of the real-time control algorithm of the parallel HEV and also the key technology in which many researchers are engaged.

Remaining difficulties of the design for the real time control strategy lie in many aspects. First, the charge of the reversible energy source must be sustained without external sources, but based only upon fuel conversion or regenerative braking during the vehicle operation. Second, no or very limited prior knowledge of the future driving condition is available during the actual operation and the driver's operation changes due to the varying environment at driving [3]. The last, the hybrid powertrain, which is comprised by the engine, electric motor, power battery, automatic mechanical transmission (AMT) etc, is a nonlinear dynamic integrated system of electrical, mechanical, chemical and thermodynamic devices. Making these devices operate effectively results in the complexity of the controlled plant [4, 5].

Much research work addressed to the control strategy of parallel HEV has been conducted in recent years. They can be roughly classified into three categories. The first type employs heuristic control techniques such as logic threshold /fuzzy logic /neural networks for estimation and control algorithm development; the second type is instantaneous optimization control strategy based on real-time computation of the equivalent fuel consumption and emission at possible operating points. The third type employs global optimization techniques such as dynamic programming, mathematic programming, and optimization

algorithms based on classical variational approach. Control strategies that are based on the minimization of the fuel consumption seem to be one step ahead of heuristic control strategies that are based upon simple rule and maps. The former, also known as optimal controllers in fact provide more generality and reduce the need for heavy tuning of the control parameters. Global optimization techniques are not implementable in real-time control because they require a priori known driving cycle. They are currently using as a basis of comparison for evaluating the quality of other control strategies. Contrary to the Global optimization method, not requiring a priori knowledge of the future driving conditions makes the instantaneous optimization applicable in real-time control.

In this paper, an original control strategy, which mainly composed of torque distribution strategy and instantaneously optimization algorithm for real-time control parallel hybrid electric urban bus (PHEUB) is put forward based on the analysis of energy consumption characteristics of the HEV components. The aim of the control strategy is to achieve acceptable vehicle performance and drivability requirements while simultaneously maximizing the engine fuel economy and maintaining the battery state of charge (SOC) in its operational range at all times.

The remainder of this paper is organized as follows: In Section 2, the powertrain system's configuration and the parameters of the specific PHEUB investigated are briefly described. Then, development of the control strategy applied in this research is presented in Section 3. Next, simulation results for minimum fuel consumption are given in Section 4. Finally, our conclusions are presented in Section 5.

2 System Configuration

The specific PHEUB powertrain system considered in this paper is designed with a diesel engine, which functions as the main power source, and an AC electric motor serves as a secondary power source. The motor is installed before the transmission. The schematic diagram of the PHEUB powertrain is shown in Fig.1. Both the output torque of the engine and that of the motor are coupled into the torque coupler, whose output torque is then transmitted into AMT through which the vehicle is propelled in the end. Gear shifting process is controlled by the AMT controller independently. There is a one-way clutch locating between the engine and the torque coupler. The parameters of main components of the PHEUB powertrain system are listed in Table 1.

Table 1Basic vehicle parameters

Parameter Name	*Parameter Value*
Engine Displacement (L)	3.9Litre Euro III
Engine Peak Power (kW @ r/min)	110kW @ 2100-2500
Engine Peak Torque (Nm @ r/min)	550Nm @ 1200-1700
Engine Idle Speed (rpm)	700-800
Type of Motor	AC Asynchronous Motor
Nominal Power of Motor (kW)	45
Peak Power of Motor（KW）	125
Maximum Torque of Motor (Nm@r/min)	±630 @ <1100
Maximum Speed of Motor (r/min)	6000
MH-Ni Batteries Capacity (Ah)	55
MH-Ni Batteries Nominal Voltage (V)	312
Automatic Transmission	5 speed
Tyre Rolling Radius (m)	0.508
Vehicle Curb Weight (kg)	11140

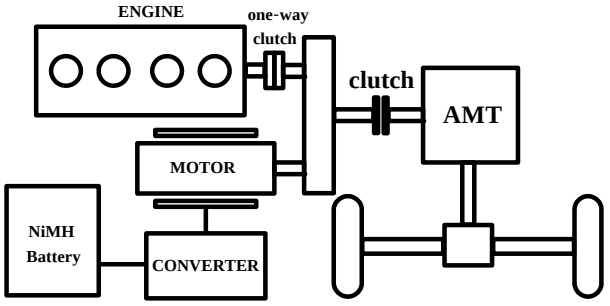

Fig.1 Schematic diagram of the PHEUB Powertrain

3 Vehicle Modeling

Because of the complexity nature of the engine, motor, battery, AMT and other subsystems, using only analytic method makes it hard to describe the operation process of each component stated above accurately and thoroughly. A complete analytic model will require considerably heavy computation. Moreover, simplifications and hypothesis used to establish the analytic model will reduce the model accuracy and make it have no superiority over the purely empirical models. Therefore, a modeling method combining theoretic analysis and experimental data is adopted for current PHEUB research [6~9]. The concept of this method that the performances of the powertrain's key components such as engine, motor and battery etc are mainly

depicted by their experiment data, and vehicle dynamic equation is still established using analytic method. In another word, it is essentially a quasi-linear model based on three-dimensional performance map. Hybrid powertrain bench test is carried out on the test bed to attain key component testing data. Under the environment of Matalab/Simulink, a feed-forward simulation model whose block diagram shown in Fig.2 is developed based on the powertrain system (showed in Figure 1) and the control strategy (described in section 4).

The simulation process is described as the followings: during each single simulation step, at first, the driver model compares the vehicle velocity requested by test drive cycle with the actual vehicle velocity feed back by the vehicle simulation model. The difference between the two speeds is calculated and used to generate commands for acceleration pedal and brake pedal. Then, these two commands alone with other vehicle information such as battery SOC, current gear location and status of clutch are all sent to vehicle controller unit (VCU) model for optimization calculation. After that, the control algorithm sends out drive commands to motor and engine, engage command and shift gear command to AMT. Finally, by applying model of engine, motor and transmission system, and the vehicle dynamic equation, the actual vehicle speed and battery SOC are calculated and then feed back to the driver model and the VCU model for next step calculation.

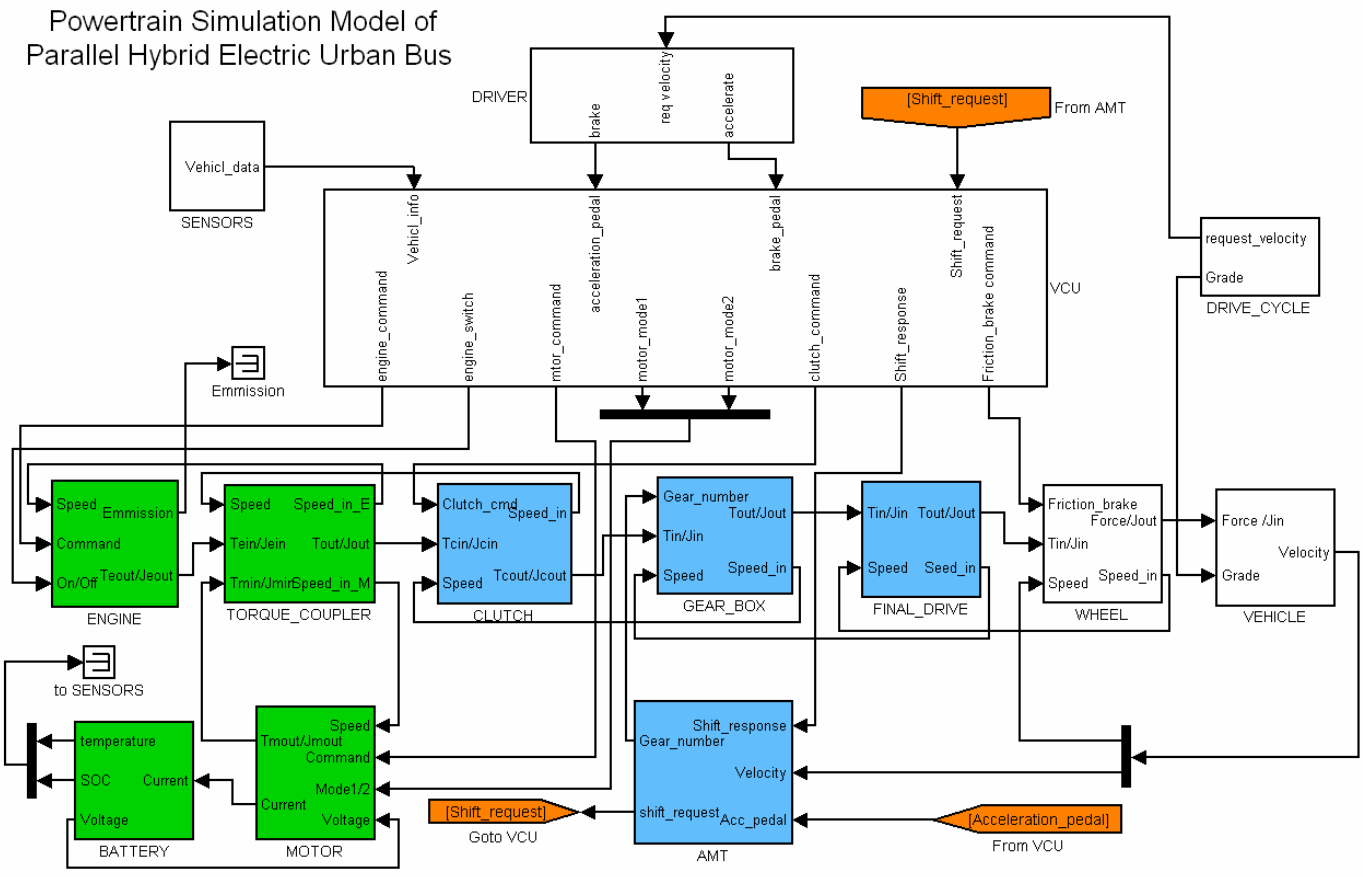

Fig.2 Diagram of PHEUB simulation model

3.1. Diesel Engine Model

The objective of the engine control is to control the engine operate at its high efficiency region as much as possible, which is realized by commanding the exdogeous control variables such as the control of fuel feeding system for the diesel engine [5]. In this works, it is a singnal named as accelerator pedal (AP) position wrapped in a CAN message which is sended by VCU to engine module controller (EMC) [10, 11]. The endogenous control variables, such as exhaust gas recirculation, air-to-fuel ratio (A/F) etc are regarded as precalibrated control variables and not considered in modeling. Therefore, the main task for engine modeling is to establish the relationship between fuel control command and torque output of the engine, and the model of the engine's fuel consumption (emmission is not considered in this paper). Fig.3 shows the inputs and

outputs of the diesel engine model. The output parameters are engine torque T_e, inertia J_e, fuel consumption Q_e and the emissions (CO, HC, NOx), while the input parameters are fuel control command β_e ([0,1]), enine start/stop singnal E_S and the engine speed n_e which is calculated from the transmission system.

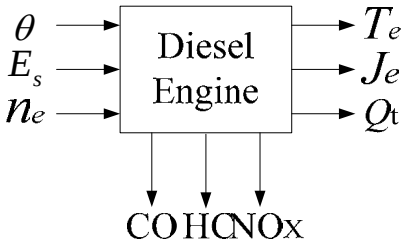

Fig. 3 Inputs and outputs of the diesel engine model

The engine output torque is discribed as:

$$T_e = f(\theta, n_e) \quad (1)$$

The fuel consumption is described as:

$$Q_e = \int_0^t \dot{Q}_e dt = \int_0^t Q_e(T_e, n_e)\mathrm{d}t \quad (2)$$

Where $f(\cdot)$ and $Q_e(\cdot)$ are two-dimensional look-up table functions. Based on the test data, the engine model is construced by establishing the relationship of the engine fuel control command β_e versus engine speed and torque as well as the fuel consumption versus engine speed and torque. The actual value of both the engine output torque and the fuel consumption are calculated from the engine model using the method of two-dimentional lookup table as well as sectional quadratic spline interpolation. Fig.4 shows the fuel consumption characteristics of the engine.

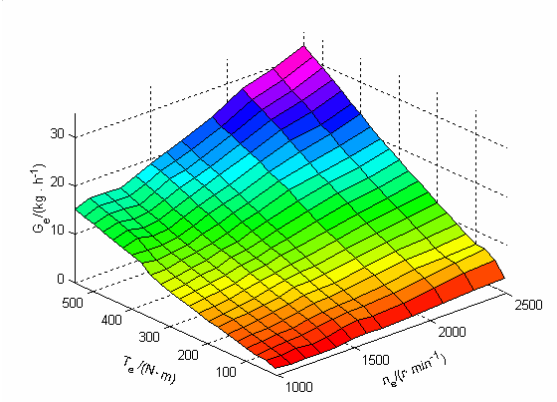

Fig.4 The fuel consumption characteristics of engine

3.2. Electric Drive Model

The electric drive system comprises an AC electric motor, an inverter and a motor controller. The motor controller is responsible for regulating the motor torque to meet the torque request commanded by the VCU. The voltage control signals produced by the motor controller are sent to the inverter to generate three-phase PWM voltage, which is used to manipulate the AC motor.

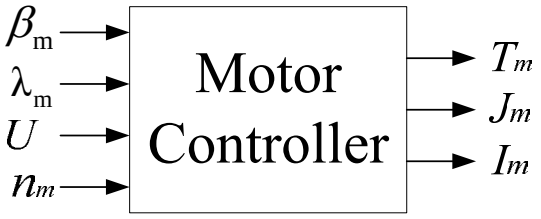

Fig.5 Inputs and outputs of the motor/controller model

In some previous research [12~15], an electromagnetic dynamic model of equivalent circuit was proposed for the investigation of motor's transient behavior thoroughly. However, time-consuming requirement of the detailed model makes it not suitable for driving-cycle-based vehicle simulation. Therefore, an empirical map-based model is used in this study. The AC Electric motor, inverter and motor controller are regarded as a single system for modeling. Fig.5 shows the input and outputs of the motor model. The input parameters are motor torque command β_m ([0,1]), motor operating mode command λ_m (drive mode, charging mode, racing mode, and speed regulating mode), the bus voltage of the electric source U and the motor speed nm, which is calculated from the rotational dynamic equation in the vehicle model. The output parameters are motor actual output torque T_m, inertia of the rotor shaft J_m and the inverter current I_m. Under the control of the drive mode, the motor output torque T_m is described as :

$$T_m = \beta_m \cdot T_{m\_max} \quad (3)$$

Where T_{m_max} is the maximum torque the motor can generate and it is a function of rotational speed and temperature. The motor can operate at peak power for a short period of time. With increasing temperature of the motor, there is a requirement of reducing power output to maintain thermal balance of the motor.

$$T_{m\_max} = f(n_m, t_m) \quad (4)$$

Except for the performance limitation imposed by itself, T_{m_max} is also limited by both the voltage U

and the maximum electric current $I_{\text{m\_max}}$. Therefore, under the driving mode the $T_{\text{m\_max}}$ is determined by the following equation:

$$T_{\text{m\_max}} = \min\left(f(n_{\text{m}}, t_{\text{m}}), \quad 9.55\frac{UI_{\text{m\_max}}}{n_{\text{m}}} \right) \tag{5}$$

If the motor works under the charging mode then $T_{\text{m\_max}}$ can be expressed as:

$$T_{\text{m\_max}} = \max\left(f(n_{\text{m}}, t_{\text{m}}), \quad 9.55\frac{UI_{\text{m\_max}}}{n_{\text{m}}} \right) \tag{6}$$

The motor electric current I_{m} can be calculated from the following equations:

$$I_{\text{m}} = \frac{P_{\text{m}}}{U} \tag{7}$$

$$P_{\text{m}} = \begin{cases} T_{\text{m}} n_{\text{m}} / \eta_{\text{m}} & T_{\text{m}} \geq 0 \\ T_{\text{m}} n_{\text{m}} \cdot \eta_{\text{m}} & T_{\text{m}} < 0 \end{cases} \tag{8}$$

where P_{m} is the motor input(driving mode) or output (charging mode) power, η_{m} is the motor efficiency regarding speed and torque and it is obtained by conducting motor performance test. It can be expressed as:

$$\eta_{\text{m}} = f(T_{\text{m}}, n_{\text{m}}) \tag{9}$$

where $f(\cdot)$ is two-dimentional look-up table function depending on the motor output torque and the motor rotational speed which are shown in Fig.6.

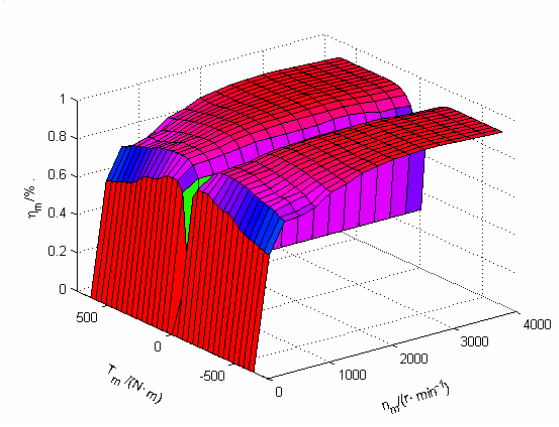

Fig.6 The efficiency characteristics of motor

3.3. Battery model

The same method is adopted for battery modeling in this research. Fig.7 shows the input and outputs of the battery model. The input parameter is battery current I_{B}, and output parameters are battery state of charge S_{C}, battery output voltage U_{oc} and battery temperature t_{B}. The battery model employs the internal resistance model addressed by literature [16], the battery internal resistance model is comprised by two sub-model, one is electrical model and the other is thermal model. (Thermal model is not considered in this paper). The electrical model shown in Fig.7 is used to represent battery operation. The equivalent internal resistance R_{int}, and the open circuit voltage U_{oc} are lumped representations of complex chemical process.

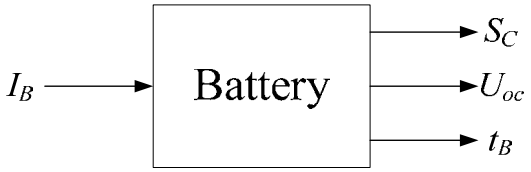

Fig.6 Input and outputs of the battery model

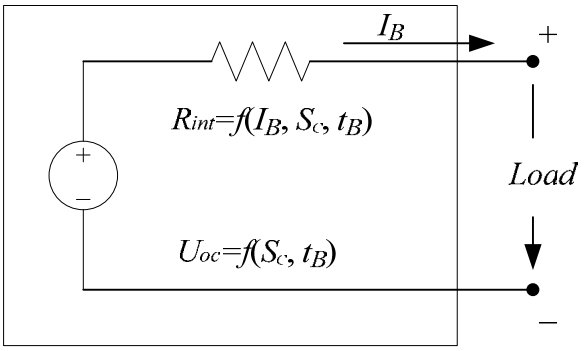

Fig.7 Classical equivalent model for the batttery

Battery internal resistance R_{int} is a function of battery temperature, battery SOC and battery current direction, it can be calculated from the following equation:

$$R_{\text{int}} = f(I_{\text{B}}, S_{\text{C}}, t_{\text{B}}) \tag{10}$$

The open circuit voltage U_{oc} is the function of battery SOC and battery temperature, and it can be expressed as:

$$U_{\text{oc}} = f(S_{\text{C}}, t_{\text{B}}) \tag{11}$$

where $f(\cdot)$ is a two-dimentional lookup table function incorporating with interpolation function. Both the relationship of battery internal resistance for charging or discharging with battery SOC, battery temperature as well as battery current and that of battery open circuit voltage with battery SOC and battery temperature are lookup table based on test data.

The battery SOC is calculated by using the equation:

$$S_{\mathrm{C}} = S_{\mathrm{init}} - \frac{\int I_{\mathrm{B}} \cdot \mathrm{d}t}{Q_{\mathrm{B\_CAP}}} \tag{12}$$

where $Q_{\mathrm{B\_CAP}}$ is the maximum battery charge, S_{init} is the initial value of battery SOC before simulation. Experimental data of the battery illustrated in Fig.8 are all used to calculate U_{oc} and R_{int} . Fig.8 (a) shows the battery pack open circuit voltage. Fig.8 (b) and Fig.8 (c) illustrate the charging and discharging resistance of the battery respectively.

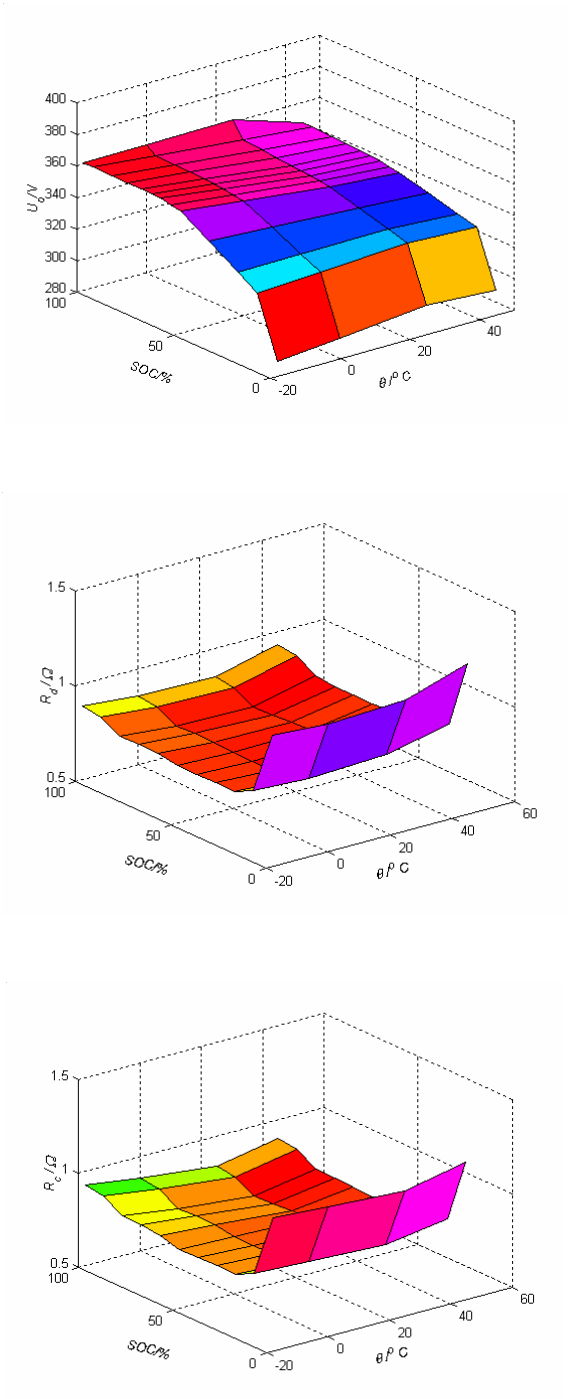

Fig. 8 U_o , R_d and R_c characteristics of battery pack

3.4. Vehicle controller unit (VCU) model

The functions of VCU are to accept driver command and monitor the whole vehicle operating status simultaneously. Its output commands calculated by the control algorithm are used to manipulate the hybrid system executing the corresponding action. The Simulink model of the vehicle controller is shown in Fig.9, it consists of the input module, the output module and the control algorithm module, which is the kernel of the VCU model. The source code of the control algorithm is written in standard C program language and wrapped by Simulink S-Function. Therefore, the control code can work after being compiled and transferred to the real controller without any modification.

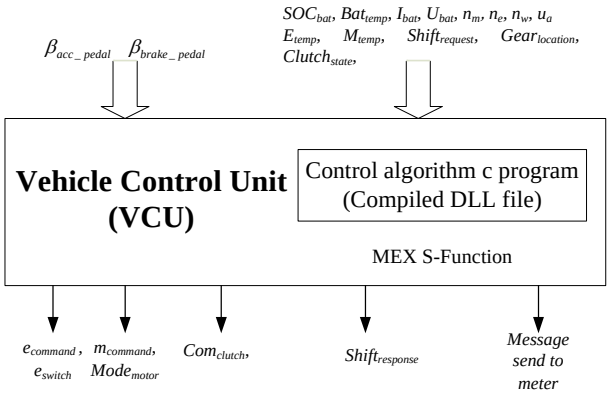

Fig.9 Vehicle controller model

3.5. Driver model

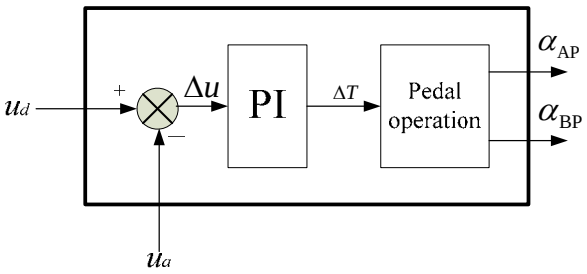

Fig.10 Input and outputs of the driver model

The driver model designed is actually a vehicle speed controller, which is shown in Fig.10. The driver model adopted a proportional-integral (***PI***) controller, through which the speed error Δu between the current vehicle speed and the desired speed is converted to the command of acceleration pedal α_{AP} or the command of brake pedal α_{BP} . The two pedal commands are then sent to the VCU controller model. The parameters of the

driver model include mainly driver's body weight G_{driver} , and the parameters depicting driver's steering style *P* and *I*.

3.6. Vehicle longitudinal dynamics model

Since vehicle dynamics and fuel economy performance are cared in this research (emissions is not considered here). Therefore only vehicle longitudinal dynamics model is involved in vehicle dynamic modeling which consists of driving and braking. Vehicle performance such as vibration and steering stability is not considered. Vehicle longitudinal dynamics model consists of wheel rotational model and vehicle motion dynamic model.

3.6.1 wheel rotational model

The input parameters of the wheel Rotational model consists of friction brake torque command κ (0~1), input torque T_{in} (N.m)and moment of inertia J_{in} (kg.m2) delivered from drive system as well as the vehicle velocity feedbacked from the vehicle motion dynamic model u_{a} (m/s).

Since only vehicle longitudinal dynamics is concerned, there is no requirement of considering the distribution of the brake torque between the front wheel and the rear wheel. The tire longitudinal force F_{t} is calculated by the following equation:

$$F_{\text{t}} = \frac{T_{\text{in}} - \kappa \cdot T_{\text{f\_max}}}{R} \tag{13}$$

The tire adhesion coefficience can be expressed as:

$$\mu = F_{\text{t}} / F_{\text{z}} \tag{14}$$

Where $T_{\text{f\_max}}$ is the total maximum friction brake torque of the front wheels and rear wheels; R is wheel radius; whenever $F_{\text{t}} > 0$ the vehicle is under driving; $F_{\text{t}} < 0$ the vehicle is under braking; F_{z} is the tire normal force. Fig.11 shows an adhesion-slip curve for some dry road surface which referenced from literature of vehicle dynamics, the wheel slip s can be estimated based on the value of μ from the figure.

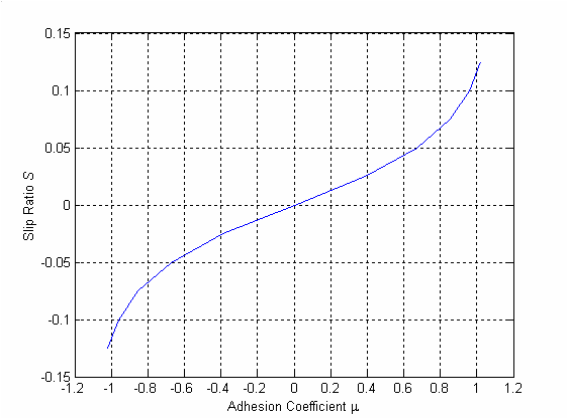

Fig.11 Adhesion-slip curve for dry road surface

Wheel speed n_{w} is calculated as:

$$n_{\text{w}} = (1+s)\frac{u_{\text{a}}}{R} \tag{15}$$

The equivalent translational mass of vehicle rotating components M_J (kg) can be calculated by using the following equation:

$$M_{\text{J}} = \frac{(1+s)\cdot J_{\text{r}}}{R^2} \tag{16}$$

Where J_{r} is the equivalent moment of the inertia of rotating components including the engine, motor, clutch, gearbox, axle and wheels in the vehicle. It can be expressed as:

$$J_{\text{r}} = [\, J_{\text{E}} i_{\text{g}} i_0 \quad J_{\text{M}} i_{\text{tc}} i_{\text{g}} i_0 \quad J_{\text{TC\_CI}} i_{\text{g}} i_0 \quad J_{\text{CO\_TI}} i_{\text{g}} i_0 \quad J_{\text{TO}} i_0 \quad J_{\text{D}} \quad J_{\text{W}} \,] K^{\text{T}} \tag{17}$$

$$K = [\, S_1 S_2 \quad S_1 S_2 \quad S_1 S_2 \quad S_2 \quad 1 \quad 1 \quad 1 \,] \tag{18}$$

where J_{E}、J_{M}、$J_{\text{TC\_CI}}$、$J_{\text{CO\_TI}}$、J_{TO}、J_{D}、J_{W} is rotary inertia of the engine, motor, torque coupler and clutch input shaft, clutch output shaft and transmission input shaft, transmission output shaft, final drive, wheel repectively; S_1 is the engage status of clutch, $S_1 = 1$ clutch engaged, $S_1 = 0$ clutch disengaged; S_2 is the gear location of the gearbox, $S_2 = 1$ gearbox is on, $S_2 = 0$ gearbox is off ; i_{g}、i_0、i_{tc} is the ratio of gearbox、final drive and torque coupler respectively.

3.6.2 vehicle motion dynamic model

Input parameters of the vehicle motion dynamic model are vehicle traction force F_{t} (N), road grade angle α and the equivalent translational mass of vehicle rotating components M_{J} (kg), output parameter is vehicle velocity u_a (m/s). The vehicle

acceleration is yielded from the vehicle traction force by overcoming the grade force, aerodynamic drag force and the rolling resistance force.

The grade force F_{p} is expressed as:

$$F_{\mathrm{p}} = Mg\sin(\alpha) \tag{19}$$

The aerodynamic drag force F_{w} is expressed as:

$$F_{\mathrm{w}} = 0.5\rho_{\mathrm{a}} C_{\mathrm{D}} A u_{\mathrm{a}}^{\ 2} \tag{20}$$

Where A is the frontal area of the vehicle (m^2), C_{D} is the aerodynamic drag coefficient, ρ_{a} is the density of air (kg/m3).

The rolling resistance force F_{r} is calculated by the following equation:

$$F_{\mathrm{r}} = Mg\left\{ f_0 + f_1(\frac{u_a}{27.78}) + f_4\left\{\frac{u_a}{27.78}\right\}^4 \right\}\cos(\alpha) \tag{21}$$

The longitudinal vehicle acceleration is expressed as:

$$a = \frac{F_{\mathrm{t}} - F_{\mathrm{p}} - F_{\mathrm{w}} - F_{\mathrm{r}}}{M + M_{\mathrm{J}}} \tag{22}$$

where M is the vehicle total mass(kg), therefore the velocity can be integrated from the following equation:

$$u_{\mathrm{a}} = \int_0^t \mathrm{adt} \tag{23}$$

4 Control Strategy

4.1 Logic threshold torque distribution strategy

According to the torque requested by the driver, the torque distribution strategy should be analyzed for two different situations:

(1) The torque requested by the driver is negative which means that the vehicle is under braking. The motor recovers the maximum possible regenerative braking energy within the constrains imposed by the motor, the battery, the brakes and vehicle stability considerations. The brakes only supply whatever is left over.

$$T^{req} = T_b + T_m^{req} \tag{24}$$

Where T^{req} is the torque requested by the driver, $T_b (\le 0)$ is the required torque for the hydraulic-brake system to deliver, $T_m^{req} (\le 0)$ is the required torque for motor to supply, and the motor torque is constrained by the battery security as well as the motor capability.

(2) The torque requested by the driver is positive which means that the vehicle is under the driving process; the requested torque is distributed between the engine and the motor:

$$T^{req} = T_e^{req} + T_m^{req} \tag{25}$$

Where T^{req} is the torque requested by the driver, T_e^{req} is the torque required for the engine to deliver. T_m^{req} is the required torque for motor to supply.

Since all the energy of parallel HEV eventually comes from the engine, the control strategy should keep the engine working at its high efficiency region as much as possible. Therefore, a couple of engine working curves should be predefined for the engine control [17, 18]: the engine maximum torque curve $T_e^{\max}$; the engine optimal efficiency torque curve T_e^{opt}; the engine minimum steady rotary speed working curve $n_e^{\min}$; the engine minimum operating torque curve T_e^{off}, The predefined working curves are shown in Fig.12.

In order to guarantee the efficiency as well as the security of the battery's charging and discharging performances whenever the parallel HEV is operating, the control strategy should keep the balance of the battery SOC. There are mainly two methods can be used to the battery SOC control for the parallel HEV [19, 20]:

The first method is implemented by controlling the SOC between the lower SOC limits (S_{L}) and the upper SOC limits (S_{H}), which are defined by the control strategy for the use of the battery. If the actual SOC is less than S_{L}, the battery is actively charged by the hybrid system; and if the actual SOC is greater than S_{H}, the hybrid system stops active charging as well as passive charging which is regenerated during barking and decelerating.

The second method is implemented by defining a target value of SOC (S_{T}). Whenever the SOC deviates from the S_{T}, a charge or discharge command is generated by the control strategy to control the SOC closer to the S_{T}. The more the SOC strays from its target, the higher power the battery is required.

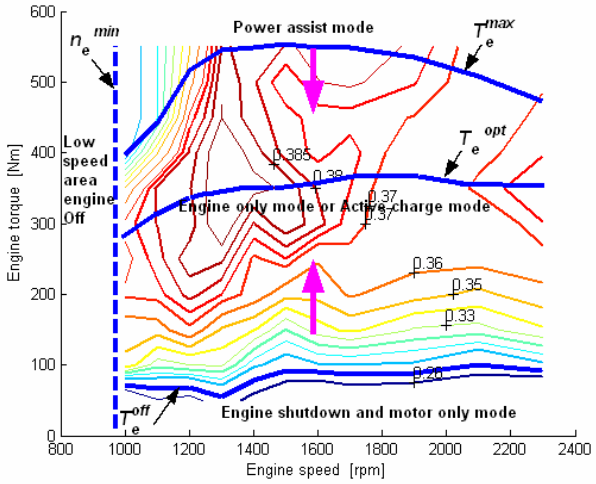

Fig.12 Torque distribution strategy for PHEUB

No matter which kind of method is used, in order to decrease the energy losses during charging and discharging process, the SOC is always controlled in the region where both internal charge and discharge resistance is relative small. The first method is selected for battery control.

Based on the defined engine working curves and battery SOC, torque distribution strategy of the parallel HEV can be generalized as following rules:

If $n_e < n_e^{\min}$, the clutch is disengaged and the vehicle is driven by the motor alone, n_e is the actual rotation speed of the engine.

Under the condition that $T^{req} < T_e^{\min}$: if battery SOC is relatively high, the motor drives the vehicle individually, and $T_e^{req} = 0$; if battery SOC is relatively low, the engine drives the vehicle and provides excess charge torque, which passes through the motor to charge the battery for keeping the balance of battery SOC and enhance load rate of the engine for improvement of the fuel economy, and $T_m^{req} < 0$.

Under the condition that $T_e^{\min} < T^{req} < T_e^{\max}$: if battery SOC is relatively low and there is torque left for the engine besides meeting the torque requested by the driver, the battery is charged by feeding these residual torque to motor; if battery SOC is relatively high, the vehicle is just driven by engine alone, then $T_m^{req} = 0$.

Whenever $T^{req} > T_e^{\max}$, which means the engine torque available can not meet requirement of the torque request from driver, the engine drives the vehicle at maximum torque $T_e^{\max}$ and the motor is activated to make up the difference ($T^{req} - T_e^{\max}$) for assistant driving.

According to the operating modes of both the engine and the motor, there are altogether six steady operating modes for the parallel HEV: (a) the vehicle starting up electrically and driven by the motor alone, (b) the vehicle driven by the engine alone, (c) the engine driving the vehicle with the motor assisting in parallel at full acceleration, (d) the engine driving the vehicle and the motor charging the battery simultaneously, (e) regenerative braking, (f) vehicle stopping or coasting. The operating modes and the energy flows of the hybrid powertrain system are shown in Fig.13. The hybrid vehicle switches between the above six operating modes during driving. Which mode the system should be working at is determined by the VCU according to the driver's accelerator pedal command, shift position, brake pedal effort, current vehicle speed, battery SOC and other vehicle state information. Since the logic threshold torque distribution strategy is basically a rule-based control strategy, the hybrid system enters into the corresponding mode when a certain condition is satisfied. For example, under the condition that the acceleration pedal is pressed slightly, while the vehicle speed is low enough and the battery SOC is high enough, the system operates in electrical driving mode.

Despite of the advantages, such as that it is simple and easy to be implemented, does not require many lines of code, and computationally efficiency and robust, the logic threshold torque distribution strategy appears to have some drawbacks such as the ability to optimize the vehicle performance is limited, the engine often operates at non-optimal efficiencies and the charging of the battery is performed at times without consideration the loss paths for the particular operating point. Since the control strategy would not necessarily result in a balance of battery SOC, the battery would probably be charged or discharged over time, and the controller would eventually have to switch to a charging or discharging mode forcibly to restore the battery charge. The overall efficiency of the hybrid system will be compromised, even though the overall efficiency before is relatively high.

In order to overcome these drawbacks and make the hybrid system work in the maximum overall efficiency, an instantaneously optimization algorithm is introduced to rectify the logic threshold torque distribution strategy; the purpose is to keep the balance of battery SOC and utilize the vehicular energy more effectively than it did before.

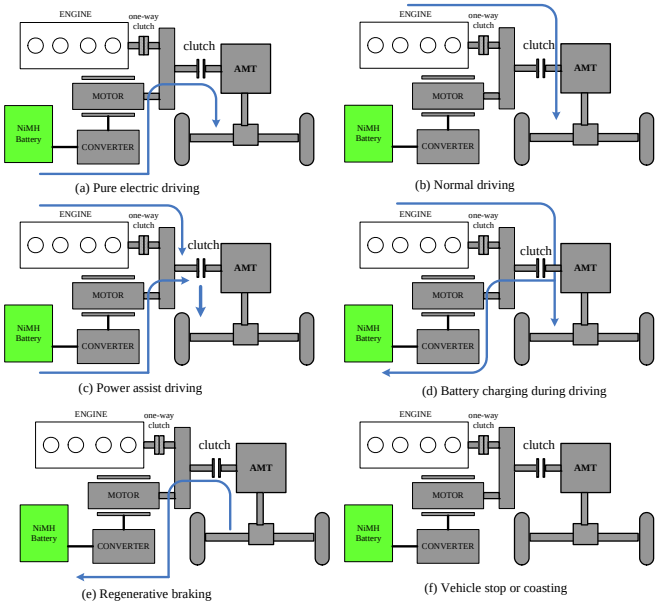

Fig.13 Typical operating modes and energy flows of the hybrid powertrain system

The schematic diagram of the control flow for the current control strategy is shown in Fig.14. At first, the logic threshold torque distribution strategy determines the operating mode based on the feedback vehicle information such as vehicle actual speed, engine actual speed, motor actual speed, battery SOC, gear location and clutch status as well as the sampled A/D information from the acceleration pedal, braking pedal and the gear shift handle which represents the driver's intention. Since the object of optimization is the engine operating points, once the system enters into the operating modes (b), (c) and (d) where the engine is tart part in driving, the instantaneous optimization algorithm is applyed to calculate the optimal hybrid system operating points. After that, the optimal control commands are sent to each part of the hybrid powertrain to complete the corresponding control.

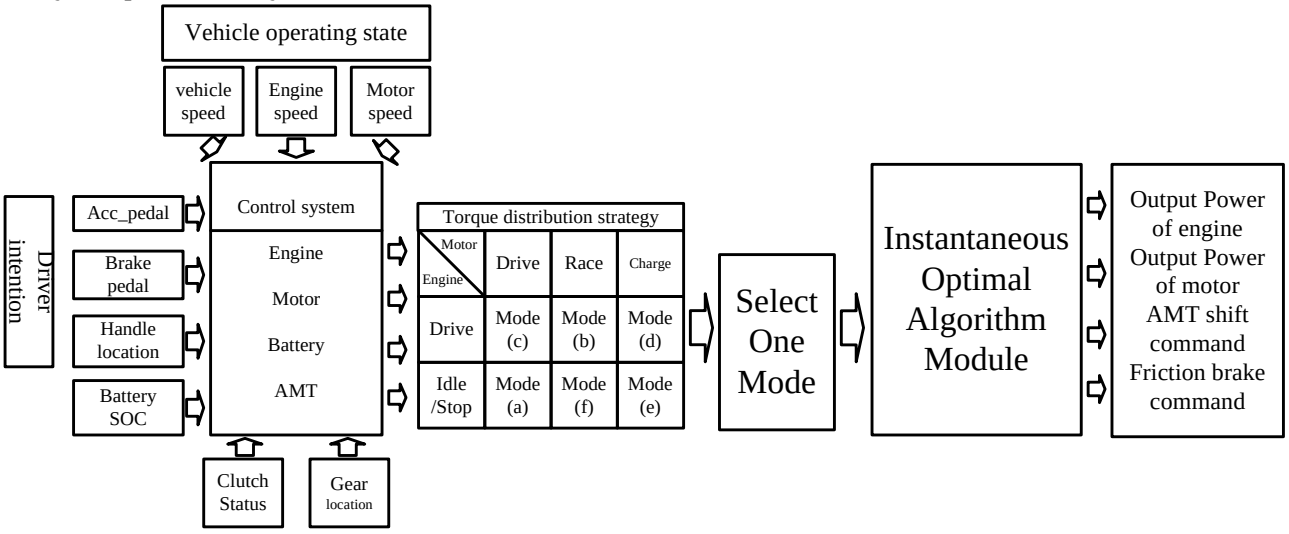

Fig.14 Implementation of the proposed control strategy controller in applied PHEUB

4.2 Instantaneous optimization algorithm

The energy consumed by the HEV is eventually come from the fuel consumption, therefore the total energy consumed by the engine and the motor can be expressed by the requirement of the fuel consumption. Since the parallel HEV encompasses two energy storage sources and associated energy converters, power system not only consumes the fuel directly but also indirectly expends the fuel by consuming battery electricity energy; The key element for calculating fuel consumption of power system is to obtain the equivalent fuel consumption corresponding to the battery electricity energy.

4.2.1 Fuel consumption of the engine

According to the engine speed and engine torque, the actual fuel consumption can be calculated by using equation (2).

4.2.2 Equivalent fuel consumption of the motor

The battery electricity energy generated or consumed by the motor equals to a mount of fuel energy. Since the energy stored in battery cannot be calculated directly from the fuel consumption energy, several approaches can be used to calculate the equivalent fuel consumption of battery electricity energy, such as the method of the fixed coefficient and the other equivalent fuel consumption calculation methods. For the fixed coefficient method, the fixed equivalent coefficient

(8.824kw.h/L) referenced from SAEJ1711[21] is used for calculation. However, the inherited deficiency of this method is that it does not consider the application range for different types of vehicle and the effects of components comprising such vehicles, the operating state of the HEV are not taken into account either. Therefore, using fixed coefficient to calculate the equivalent fuel consumption would result in large error. In the Real-time Control Strategy [22] for the calculation of the motor equivalent fuel consumption, the effects of the losses during charge or discharge, the free electrical energy obtained from regenerative braking and battery SOC as well as the variation of SOC in a single sample step ΔSOC are all taken into account to calculate the instantaneous equivalent fuel consumption. Finally, the instantaneous equivalent fuel consumption based on current vehicle operating mode is obtained. However, this method not only requires lots of computation but also needs real-time calculation while the parallel HEV is running which makes it hard to apply in real controlling system. During the operating process of the parallel HEV, the efficiency of the engine driving motor to charge battery cannot be kept at a constant value. However, an appropriate control strategy can be utilized to avoid low efficiency operating point and make the hybrid system working at a higher efficiency range. Therefore, it is feasible to use the mean efficiency of the engine driving motor to charge the battery and take the free regenerative braking energy into account as well for the calculation of the equivalent fuel consumption corresponding to battery electricity energy. Based on the information of vehicle such as the gear number n, vehicle speed u_a, battery SOC, torque of the engine T_e and the motor T_m, the equivalent fuel consumed by the motor can be calculated according to the following steps:

(1) Determining working range of the motor T_{m}. The maximum of T_{m} is determined by the greatest possible motor torque $T_{\mathrm{m\_p}}$ and the minimum is determined by the greatest possible negative motor torque $T_{\mathrm{m\_n}}$.

$T_{\mathrm{m\_p}}$ is the minimum of the following three:

① driver requested torque at the engine shaft T_{r};

② the maximum positive torque of the motor at the current speed;

③ the maximum available possible torque from the motor under the limit of the discharging capability of the battery.

$T_{\mathrm{m\_n}}$ is the maximum of the following three:

① $T_{\mathrm{r}} - T_{\mathrm{e\_max}}$, where $T_{\mathrm{e\_max}}$ is the maximum engine torque at the current speed;

② the maximum negative torque of the motor at the current speed;

③ the maximum available negative torque from the motor under the limit of the charging capability of the battery.

(2) Calculating input and output power of the motor by using the equation (8).

(3) As shown in Fig.15, power balance equation of the hybrid system is obtained by using the motor for the load of the battery, and the equation can be expressed as:

$$U_o I_b = R_{\mathrm{int}} I_b^2 + P_m \tag{26}$$

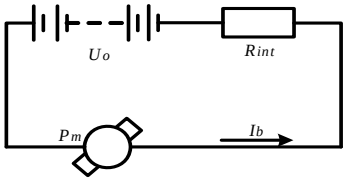

Fig.15 The circuit of electric driven system

Where P_m is the output or the input power of the motor; I_{b} is the current of the DC bus.

Based upon the power balance equation (26), the required battery power can be expressed as:

$$P_b = U_o I_b = \begin{cases} \dfrac{U_o^2 - U_o\sqrt{U_o^2 - 4R_d P_m}}{2R_d}, & T_m \geq 0 \\ \dfrac{U_o\sqrt{U_o^2 - 4R_c P_m} - U_o^2}{2R_c} & T_m < 0 \end{cases} \tag{27}$$

(4) The mean efficiency of both engine and motor are given by:

$$\left.\begin{aligned} \overline{\eta}_e &= \frac{\sum_{i=1}^{i=K} (\eta_e(i) \cdot P_e(i))}{\sum_{i=1}^{i=K} P_e(i)} \\ \overline{\eta}_m &= \frac{\sum_{i=1}^{i=K} (\eta_m(i) \cdot P_m(i))}{\sum_{i=1}^{i=K} P_m(i)} \end{aligned}\right\} \tag{28}$$

Where $\eta_e(i)$, $P_e(i)$, $\eta_m(i)$, $P_m(i)$ (i=1,……, K) are the efficiency and the power of the engine and the motor respectively; K is the size of the sample data. For the calculation of the mean efficiency, the simulation results under specific drive cycle can be used for preliminary calculation; It has been validated to be accurate by the experiences.

(5) One part of the battery energy comes from the vehicle kinetic energy recaptured by the

regenerative braking. Although the electricity energy obtained from regenerative braking cannot be predicted beforehand, it can be estimated by tracking the regenerative energy during the drive cycle and averages it over a certain time period. The average electricity energy recaptured by regenerative braking is defined as:

$$\overline{P}_{reg} = \frac{1}{K}\sum_{i=1}^{i=k} P_{reg}(i) \tag{29}$$

(6) In order to regulate the price of electricity with different SOC, a penalty function $f_{\mathrm{p}}(S_{\mathrm{C}})$ shown in Fig.16 is introduced to correct the equivalent fuel consumption of the battery [23].

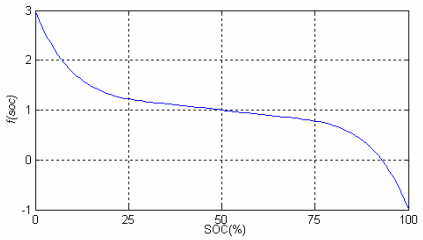

Fig.16 Penalty function for SOC correction

At the high SOC, the penalty function is small, which makes the usage of the motor/batteries less "expensive". At the low SOC, the value of penalty function increases and it becomes more "expensive" to use the batteries. Therefore the aim of penalty function is to increase the percentage of the equivalent fuel consumption consumed by motor in the overall fuel consumption whenever SOC is low, and to reduce it whenever SOC is high. The battery energy generated or consumed by motor can be expressed as:

$$Q_m = \frac{3.6(P_b + \overline{P}_{reg})}{\overline{\eta}_e \cdot \overline{\eta}_m \cdot LHV} \cdot f_p(SOC) \tag{30}$$

Where LHV (42.6x103J/g) is the lower heating value of the fuel.

4.2.3 Overall equivalent fuel consumption

By using the following equation, the total equivalent fuel consumption for each feasible candidate operating point can be calculated. The optimal operating point is the one having the minimum value.

$$Q_{total} = Q_e + Q_m \tag{31}$$

The optimization algorithm of the engine operating points is described as the following steps:

(1) Setup the fuel consumption look-up table $Q_{\mathrm{e,t}}$ indexed by the engine torque T_{e} and the engine speed n_{e}.

(2) Setup the motor efficiency look-up table $\eta_{\mathrm{m}}(T_{\mathrm{m}}, n_{\mathrm{m}})$ indexed by the motor torque T_{m} and the motor speed n_{m}.

(3) Setup battery open-voltage look-up table $U_{\mathrm{o}}(S_{\mathrm{C}}, t_{\mathrm{b}})$, battery charging look-up table $R_{\mathrm{c}}(S_{\mathrm{C}}, t_{\mathrm{b}})$ and discharging look-up table $R_{\mathrm{d}}(S_{\mathrm{C}}, t_{\mathrm{b}})$ index by battery SOC S_{C} and battey temperature t_{b}.

(4) Setup battery SOC penalty function lookup-table $Q_{\mathrm{f,t}}(S_{\mathrm{C}})$.

(5) Determine the feasible working range by using the following equation:

$$T_{\mathrm{m}} = T_{\mathrm{m,nmax}} : T_{\mathrm{s}} : T_{\mathrm{m,pmax}} \tag{32}$$

Where T_{m} is the motor output torque for each valid candidate operating point; $T_{\mathrm{m,nmax}}$ and $T_{\mathrm{m,pmax}}$ are the maximum negative and positive torque of the motor respectively; T_{s} is the calculation step of the motor torque, the smaller the T_{s} is, the better the calculation results would be; the engine torque of the corresponding operating point can be expressed as:

$$T_{\mathrm{e}} = T_{\mathrm{r}} - \rho_{\mathrm{m}} \cdot T_{\mathrm{m}} \tag{33}$$

(6) Calculate the engine fuel consumption $Q_{\mathrm{e,i}}$ for each candidate operating point by looking up the map of the fuel consumption table $Q_{\mathrm{e,t}}(T_{\mathrm{e}}, n_{\mathrm{e}})$.

(7) Calculate the motor efficiency $\eta_{\mathrm{m,i}}$ for each candidate operating point by looking up the map of the motor efficiency table $\eta_{\mathrm{m}}(T_{\mathrm{m}}, n_{\mathrm{m}})$.

(8) Calculate input or output motor power $P_{\mathrm{m,i}}$ for each candidate operating point by using the equation 3 and the result of step (7). It is noteworthy that positive motor torque generates output motor power $P_{\mathrm{m,i}}$ while negative torque generates input motor power $P_{\mathrm{m,i}}$.

(9) Calculate battery open-circuite voltage $V_{\mathrm{o,i}}$, charging resistance $R_{\mathrm{c,i}}$ and discharging resistance $R_{\mathrm{d,i}}$ by looking-up table $U_{\mathrm{o}}(S_{\mathrm{C}}, t_{\mathrm{b}})$, $R_{\mathrm{c}}(S_{\mathrm{C}}, t_{\mathrm{b}})$ and $R_{\mathrm{d}}(S_{\mathrm{C}}, t_{\mathrm{b}})$.

(10) Calculate battery current $I_{\mathrm{b,i}}$ by using equation (6) and the results of step (8) and (9).

(11) Compute battery power $P_{\mathrm{b,i}}$ generated or consumed by motor based upon the results of step (8)~(10) and equation (6).

(12) Calculate the average regenerative energy $\overline{P}_{\mathrm{reg}}$ based on the statistics of typical driving cycles

and the past driving data. $\overline{P}_{\text{reg}}$ is used to correct $P_{\text{b,i}}$ in step (11): $P_{\text{b, i}} = P_{\text{b, i}} + \overline{P}_{\text{reg}}$.

(13) Calculate the corresponding value of the SOC penalty function $Q_{\text{f,i}}$ by looking-up $Q_{\text{f,t}}(S_{\text{C}})$ based on the actual S_{C}.

(14) By using the resultes from step (12) and (13) the equivalent fuel consumption $Q_{\text{m, i}}$ corresponding to rectified battery energy $P_{\text{b,i}}$ can be calculated.

(15) Calculate the total fuel consumption for each candidate operating point: $Q_{\text{t, i}} = Q_{\text{e,i}} + Q_{\text{m,i}}$. The optimal point is the one have a minimum Q_{t}.

The flowchart of the optimization algorithm is illustrated in Fig.17.

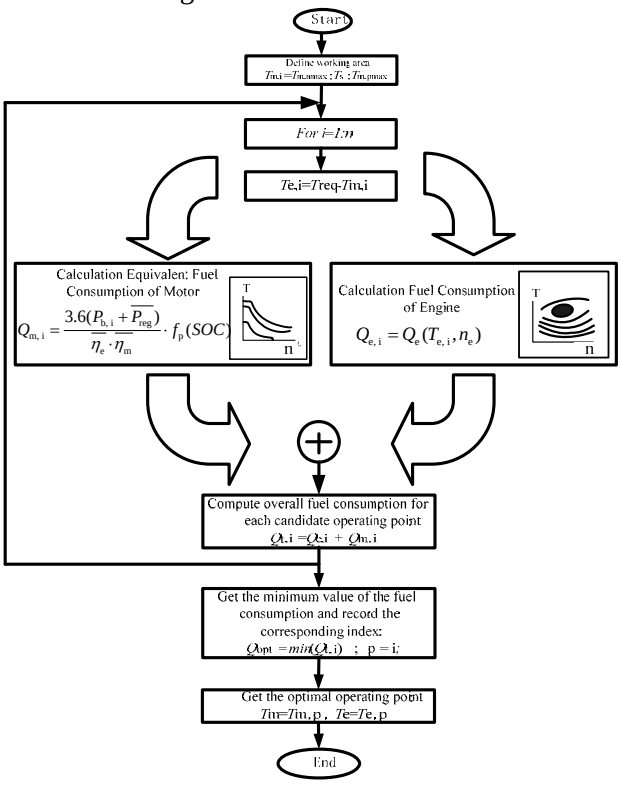

Fig.17 Flowchart of the optimization algorithm

5 Validation of The Control Strategy

A feed-forward HEV simulation model developed at Shanghai Jiao Tong University is adopted to assess the performance of the control strategy proposed in this paper. This model is implemented in Matlab/Simulink and is verified with the bench test data for an HEV prototype bus. More details of this model can be found in [9, 18].

The simulation results over the China Typical Bus Driving Schedule at Urban District (CTBDS_UD) with initial SOC value of 0.5 and 0.7 are shown in Fig. 18(a) and 18(b) respectively, which illustrate the engine torque (T_e), the motor torque (T_m) as well as the driver's request torque (T_{req}) by interpreting acceleration and brake pedal. Battery SOC and vehicle velocity variations (u_a) are also record and presented in the Figures. Fig. 18 also reveals that the SOC remains within the operational range in spite of the initial SOC.

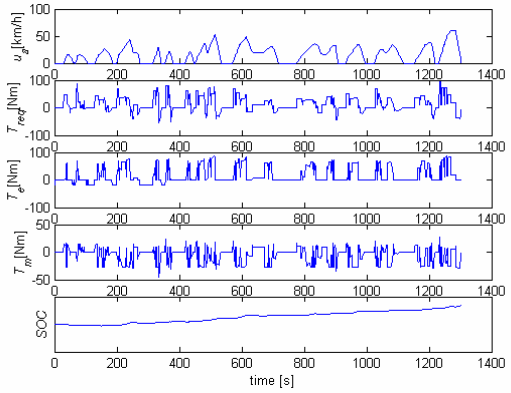

(a) With the initial SOC of 0.7

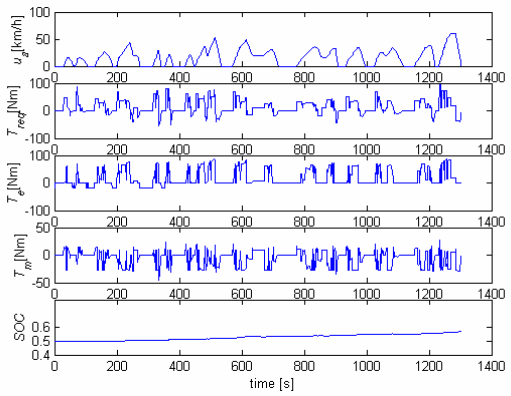

(b) With the initial SOC of 0.5

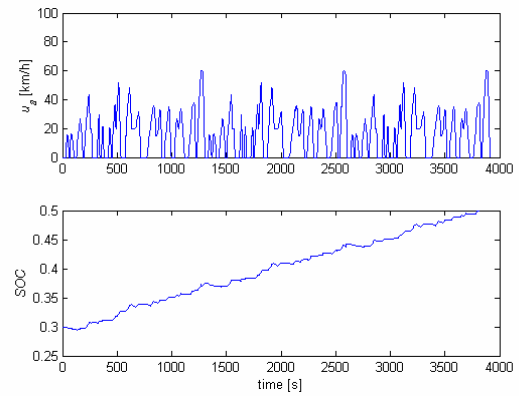

(c) Change of the SOC over a long time horizon simulation.

Fig.18 Simulation results of PHEUB on CTBDS_UD

It can be observed more clearly that the proposed control strategy works very well in maintaining the

SOC in Fig. 18(c), which presents the changes of the SOC over a long time horizon simulation (3 CTBDS_UDs). At the very beginning, the SOC is relatively low (0.3) and the control strategy uses the engine heavily to recharge the battery in addition to meeting the vehicle demand. With the raise of the SOC, the electricity usage increases. The simulation results demonstrate the effectiveness of the proposed control strategy in maintaining the SOC.

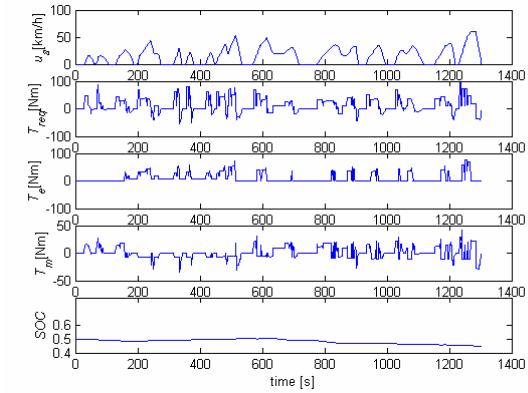

(a) With the initial SOC of 0.7

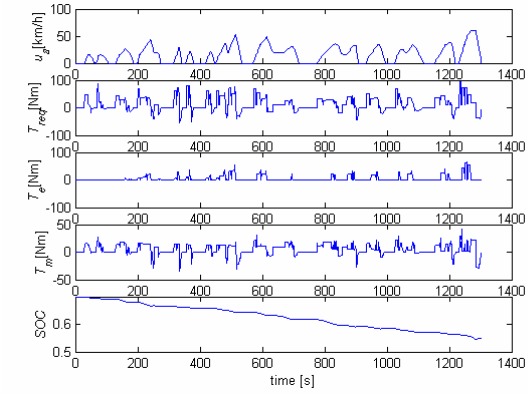

(b) With the initial SOC of 0.5

Fig.19 Simulation results of PHEUB on CTBDS_UD

Fig.19 presents the simulation results using the conventional strategy using precise parameters (LTCS). It is observed from the comparisons between Fig.19 and Fig.18 that, the engine torque is relatively higher over the cycle in Fig.18 than that in Fig.19, which means that the engine probably frequently operates in high-efficiency range. It can be also observed that the battery SOC controlled by OCS is much better than by LTCS.

For the purpose of investigating further the behavior of the engine, Fig.20 presents the engine operating points (sample time is 1s) scattered into the torque-speed plane with the initial SOC value of 0.7 for two different control strategies. One is the proposed control strategy (OCS) developed in this paper; the other is the conventional strategy using precise parameters (LTCS). The Figure's background is made up of fuel efficiency contours and the maximum torque curve of the engine. For the OCS, the operating points of the engine are more concentrated in the high efficiency range; while for the LTCS, the operating points of the engine are much more spread out over the map and many of them are in the low load and low efficiency range. This indicates that the OCS is more effective in controlling the engine operating in high efficiency range. In addition, it is necessary to explain that some of the points near the coordinate axis are not the real engine working points; They are the transition points of the engine during start or stop process, which are sampled by the simulation model.

The comparisons of the fuel economy simulation results between OCS and LTCS over CTBDS_UD are summarized in Table 2. The data in Table 3 demonstrate again that the FCS is more effective than the LTCS in keeping the engine operating at high efficiencies. Although the fuel economy for the LTCS (23.25 L/100 km) is less than that for the OCS (25.12 L/100 km), the SOC drops only by 2% for the FCS while by 15% for the LTCS. Night sets of fuel economy and SOC change results are obtained by simulation over the same driving cycle night times with different initial SOC from 0.3 to 0.7 for each run. A linear regression is used to calculate the corrected fuel economy corresponding to the zero SOC change over the cycle. The corrected fuel economy for the OCS is 25.72 L/100 km and for the LTCS is 29.36 L/100 km. It is thus obvious that the OCS is superior to the LTCS in terms of fuel economy.

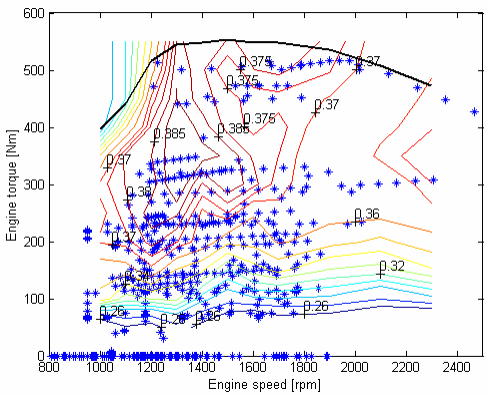

(a) LTCS

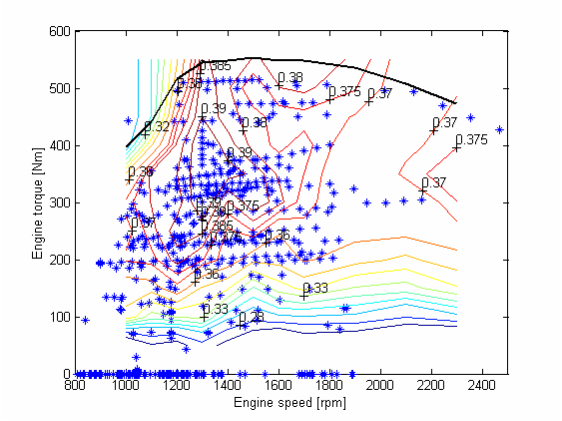

(b) OCS

Fig.20 Operating points of the engine with the initial SOC of 0.7 using (a) the LTCS (b) OTCS on CTBDS_UD.

Table 2 Fuel economy simulation results comparison between LTCS and OCS

	LTCS	OCS
Initial SOC (%)	70	70
End SOC (%)	55	68
Fuel economy (L/100km)	23.25	25.12
Fuel economy with SOC correction Q_s/(L/100km)	29.36	25.72

6 CONCLUSIONS

Real-time optimal control strategy is the key technology for PHEUB. In this paper, a novel control strategy using torque distribution strategy with the incorporation of instantaneous optimization algorithm is presented. This control strategy is developed as two steps: first, torque distribution control rules are summarized by utilizing engineering intuition and simple analysis of component efficiency tables or charts; next, the instantaneous optimization algorithm is applied to conquer the inherit deficiencies of the current torque distribution strategy and therefore achieve relatively higher overall energy efficiency. Experimental data of the engine, the motor and the battery have been used for the feed-forward system model of PHEUB on the platform of Matlab/Simulink. Consequently, simulation results manifest that not only the fuel economy of PHEUB is improved significantly but also the battery SOC maintained within its operating range while satisfying the requirement of the driver. The proposed control strategy was implemented to a real experimental PHEUB control system and has been validated by large mount of vehicle field tests. In summary, the proposed method that integrating theoretical algorithm with engineering practical experiences is feasible, and the real-time control strategy presented in this paper is very effective and practical. As for the directions for future research of the optimal torque distribution control strategy for parallel hybrid electric urban buses, the function of the torque control system control (TCS) as well as vehicle stability control (VSC, ESP) should be added into the HEV control strategy, which realize the integration of the hybrid system control and the vehicle dynamic control in the end.

ACKNOWLEDGEMENT– This work was supported by the Key Technology Research for Hybrid City Bus Project of Science and Technology Commission of Shanghai China under contract No. 033012017.

REFERENCES

[1] Iwai, N., Analysis on fuel economy and advanced systems of hybrid vehicles, *JSAE Review —Society of Automotive Engineer of Japan (JSAE)* , Vol.20, No.1, 1999, pp.3-11.

[2] Morita, K., Automotive power source in 21st century. *JSAE Review—Society of Automotive Engineer of Japan (JSAE)*, Vol.24, No.1, 2002, pp.3-7.

[3] Paganelli, G., et al., General supervisory control policy for the energy optimization of charge-sustaining hybrid electric vehicles. *Special Issue of JSAEReview — Society of Automotive Engineer of Japan (JSAE)*, Vol.22, No.4, 2001, pp.511-518.

[4] Bowles, P., et al., Energy management in a parallel hybrid electric vehicle with a continuously variable transmission. *Proceedings of American Control Conference*, Chicago, USA, 2000, pp.55-59.

[5] Zhang R, et al., Control of hybrid dynamic system for electric vehicles. *Proceedings of the American Control Conference*, Arlington, USA, 2001, pp.2884-2889.

[6] Powell, B., et al., Dynamic modeling and control of hybrid electric vehicle powertrain system, *IEEE Control System Management*, Vol.18, No.5, 1998, pp.17-33.

[7] Karen, L., et al., Matlab-Based Modeling and Simulation Package for Electric and Hybrid Electric Vehicle Desing, *IEEE Transaction of Vehicular Technology*, Vol.48, No.6, 1999, pp.1 770-1 778.

[8] Markel, T, et al., ADVISOR: a system analysis tool for advanced vehicle modeling. *Journal of Power Sources*, Vol.110, No.2, 2002, pp.255-266.

[9] Pu, J., et al., Modeling and development of the control strategy for a hybrid car (In Chinese).

Journal of Shanghai Jiaotong University, Vol.38, No.11, 2004, pp.1917-1921.

[10] SAE Recommend Truck and Bus Control and Communication Network Standards J1939-71, vehicle application layer, Issued, 2000-04.

[11] ISB4/ISBe Electronic Interface Application Technical Package Manual June 2001.

[12] Shieh, H, et al., Nonlinear Sliding-Mode torque control with adaptive backstepping approache for induction motor drive, *IEEE transaction industrial application*, Vol.46, No.2, 1994, pp.380-389.

[13] Dong ,Y. H., et al., A new type compositive hybrid power system-E.T.Driver and its application in HEV. WSEAS Transactions on Systems, Vol.7, No.3, 2008, pp.203-218.

[14] Lee, Y. B., et al., Design and performance analysis of air blower system operated with BLDC motor for PEM FC vehicle, WSEAS Transaction on Systems, Vol.4, No9, 2005, pp.1573-1580.

[15] EI-Sousy, F.M., et al., Fuzzy adaptive neural-network model-following speed control for PMSM drives. WSEAS Transactions on Systems, Vol4, No4, 2005, pp.256-259.

[16] Johnson, V. Battery performance models in ADVISOR, Vol.22, No.1, 2001, pp.95-103.

[17] Niels, J., et al., Fuzzy logic control for parallel hybrid vehicles. *IEEE Transactions on Control Systems Technology*, Vol.10, No.3, 2002, pp.460-468.

[18] PU, J., et al., Fuzzy torque control strategy for parallel hybrid electric vehicles. International *Journal of Automotive Technology*, Vol.6, No.5, 2005, pp.529-536.

[19] Sasaki, S., et al., Toyata's newly developed electric gasoline engine hybrid powertrain system. *Proceedings of the Electric Vehicle Symposium. EVS14*, Orlando, Florida,USA, 1997.

[20] Fukuo, K., et al., Development of the ultra-low-fuel consumption hybrid car-INSIGHT. *JSAE Review —Society of Automotive Engineer of Japan (JSAE)*, Vol.22, No.1, 2001, pp.95-103.

[21] SAE J1711 Recommended Practice for Measuring the Exhaust Emissions and Fuel Economy of Hybrid-Electric Vehicles, Issued, 1999-03.

[22] Johnson, V. H., et al., HEV control strategy for real-time optimization of fuel economy and emissions. *SAE Technical Paper*, 2000-01-1543, 2000.

[23] Paganelli, G., et al., Control development for a hybrid-electric sport-utility vehicle: strategy, implementation and field test results. *Proceedings of the American Control Conference*, Arlington, Virginia, USA, 2001, pp.5064-5069.